Article

The pathogenicity of SARS-CoV-2 in hACE2 transgenic mice

https://doi.org/10.1038/s41586-020-2312-y

Received: 2 February 2020

Accepted: 24 April 2020

Published online: 7 May 2020

Check for updates

Linlin Bao[1,2,6], Wei Deng[1,2,6], Baoying Huang[3,6], Hong Gao[1,2,6], Jiangning Liu[1,2,6], Lili Ren[4], Qiang Wei[1,2], Pin Yu[1,2], Yanfeng Xu[1,2], Feifei Qi[1,2], Yajin Qu[1,2], Fengdi Li[1,2], Qi Lv[1,2], Wenling Wang[3], Jing Xue[1,2], Shuran Gong[1,2], Mingya Liu[1,2], Guanpeng Wang[1,2], Shunyi Wang[1,2], Zhiqi Song[1,2], Linna Zhao[1,2], Peipei Liu[3], Li Zhao[3], Fei Ye[3], Huijuan Wang[3], Weimin Zhou[3], Na Zhu[3], Wei Zhen[3], Haisheng Yu[1,2], Xiaojuan Zhang[1,2], Li Guo[4], Lan Chen[4], Conghui Wang[4], Ying Wang[4], Xinming Wang[4], Yan Xiao[4], Qiangming Sun[5], Hongqi Liu[5], Fanli Zhu[5], Chunxia Ma[5], Lingmei Yan[5], Mengli Yang[5], Jun Han[3], Wenbo Xu[3], Wenjie Tan[3], Xiaozhong Peng[5], Qi Jin[4], Guizhen Wu[3]✉ & Chuan Qin[1,2]✉

Severe acute respiratory syndrome coronavirus 2 (SARS-CoV-2) is the cause of coronavirus disease 2019 (COVID-19), which has become a public health emergency of international concern[1]. Angiotensin-converting enzyme 2 (ACE2) is the cell-entry receptor for severe acute respiratory syndrome coronavirus (SARS-CoV)[2]. Here we infected transgenic mice that express human ACE2 (hereafter, hACE2 mice) with SARS-CoV-2 and studied the pathogenicity of the virus. We observed weight loss as well as virus replication in the lungs of hACE2 mice infected with SARS-CoV-2. The typical histopathology was interstitial pneumonia with infiltration of considerable numbers of macrophages and lymphocytes into the alveolar interstitium, and the accumulation of macrophages in alveolar cavities. We observed viral antigens in bronchial epithelial cells, macrophages and alveolar epithelia. These phenomena were not found in wild-type mice infected with SARS-CoV-2. Notably, we have confirmed the pathogenicity of SARS-CoV-2 in hACE2 mice. This mouse model of SARS-CoV-2 infection will be valuable for evaluating antiviral therapeutic agents and vaccines, as well as understanding the pathogenesis of COVID-19.

In late December 2019, cases of COVID-19—which is caused by SARS-CoV-2—were identified and reported from Wuhan city (Hubei province, China), where they were linked to a seafood market at which exotic animals were also sold and consumed[1,3]. The number of confirmed cases has since soared: as of 25 February 2020, almost 78,000 cases and over 2,700 deaths were reported in China[4], and imported cases from travellers from mainland China were reported in several other countries. It is critical to establish the pathogenicity and biology of the virus for prevention and treatment of the disease.

Because SARS-CoV-2 is highly homologous with SARS-CoV, human ACE2—which is the entry receptor of SARS-CoV—was also considered to have a high binding ability with the SARS-CoV-2 by molecular biological analysis[2,5]. We therefore used transgenic hACE2 mice and wild-type mice infected with the HB-01 strain of SARS-CoV-2 to study the pathogenicity of the virus.

Specific-pathogen-free male and female wild-type ($n = 15$) or hACE2 ($n = 19$) mice of 6–11 months of age were inoculated intranasally with SARS-CoV-2 strain HB-01 at a dosage of 10^5 50% tissue culture infectious dose ($TCID_{50}$) per 50 μl inoculum volume per mouse, after the mice were intraperitoneally anaesthetized using 2.5% avertin; mock-treated hACE2 mice ($n = 15$) were used as control. Clinical manifestations were recorded from 13 mice (3 HB-01-infected wild-type mice; 3 mock-treated hACE2 mice; and 7 HB-01-infected hACE2 mice). We observed slight bristled fur and weight loss only in the HB-01-infected hACE2 mice—and not the HB-01-infected wild-type mice or mock-treated hACE2 mice—during the 14 days of observation; other clinical symptoms, such as an arched back and decreased response of external stimuli, were not found in any of the mice. Notably, the weight loss of HB-01-infected hACE2 mice was up to 8% at 5 days post-infection (dpi) (Fig. 1a).

Next, we examined viral replication and pathological changes in three mice per group at each time point; the primary organs—including heart, liver, spleen, lung, kidney, brain, intestine and testis—were collected periodically. As shown in Fig. 1b, viral loads were detectable by quantitative PCR with reverse transcription (RT–qPCR) at 1, 3, 5 and 7 dpi in the lungs of HB-01-infected hACE2 mice (but not in those of HB-01-infected wild-type mice; data not shown), and viral RNA copies reached a peak of $10^{6.77}$ copies per ml at 3 dpi. Viral RNA was also detectable at 1 dpi in the intestine of HB-01-infected hACE2 mice, which was not detected in other tissues along the timeline (Fig. 1b). Although viral loads were detectable in the intestine, no virus in the intestine was isolated at 1 dpi; we therefore speculate that the viral load detected was residual input inoculum from the nasal mucosa transferred to the intestines by

[1]Beijing Key Laboratory for Animal Models of Emerging and Remerging Infectious Diseases, Institute of Laboratory Animal Science, Chinese Academy of Medical Sciences, Beijing, China. [2]NHC Key Laboratory of Human Disease Comparative Medicine, Comparative Medicine Center, Peking Union Medical College, Beijing, China. [3]MHC Key Laboratory of Biosafety, National Institute for Viral Disease Control and Prevention, China CDC, Beijing, China. [4]Institute of Pathogen Biology, Chinese Academy of Medical Sciences, Beijing, China. [5]Institute of Medical Biology, Chinese Academy of Medical Sciences, Beijing, China. [6]These authors contributed equally: Linlin Bao, Wei Deng, Baoying Huang, Hong Gao, Jiangning Liu. ✉e-mail: wugz@ivdc.chinacdc.cn; qinchuan@pumc.edu.cn

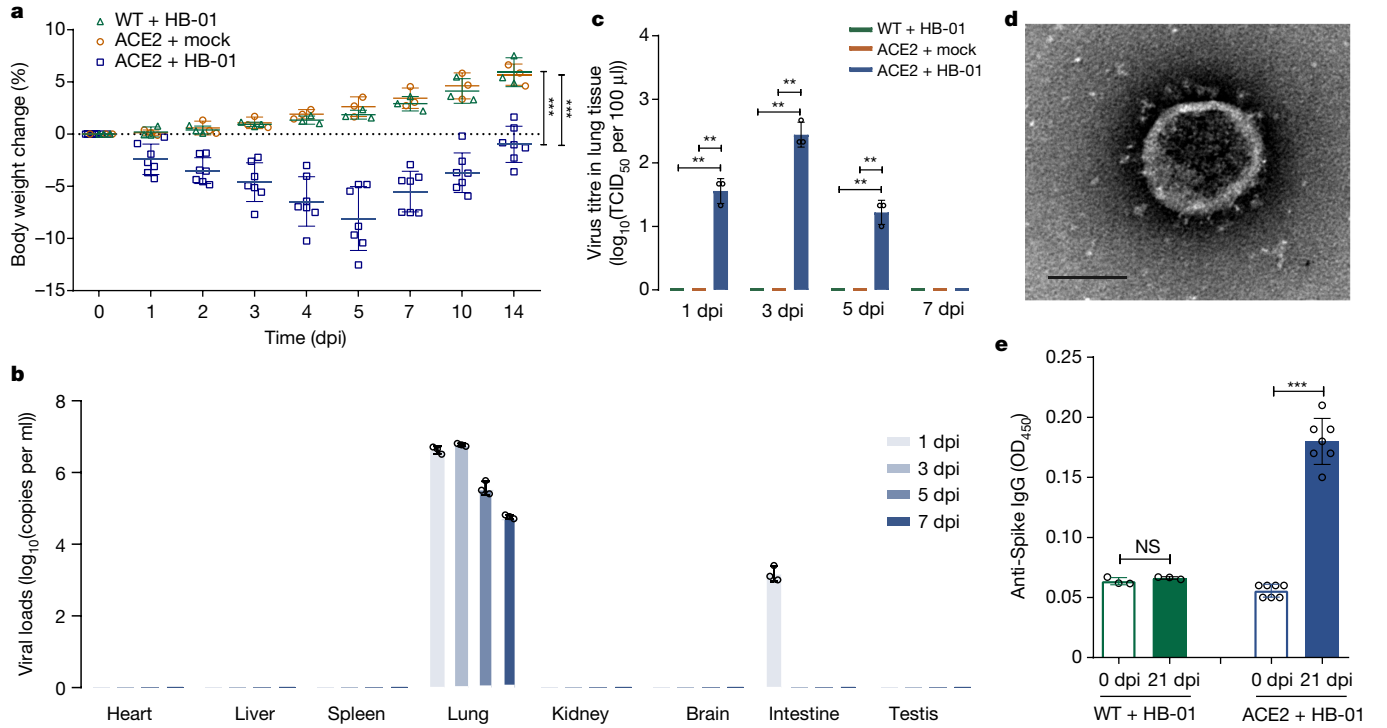

Fig. 1 | Weight loss, virus replication and specific IgG production in hACE2 mice after infection with SARS-CoV-2. a, Weight loss was recorded for 14 days. hACE2 mice ($n = 7$) and wild-type (WT) mice ($n = 3$) were experimentally challenged intranasally with SARS-CoV-2 HB-01, and mock-treated hACE2 (ACE2 + mock) mice ($n = 3$) were used as control. According to two-tailed Mann–Whitney *U*-test, the weight of HB-01-infected hACE2 mice (ACE2 + HB-01) displayed a significant decline compared with that of HB-01-infected wild-type mice (WT + HB-01) or mock-treated hACE2 mice (***$P = 0.0005$). **b**, To measure viral RNA, 12 mice were infected in each group. Three mice per group were killed, and their major organs (including testis in male mice) were collected for analysis of viral loads and virus titre at 1, 3, 5 and 7 dpi. The distribution of SARS-CoV-2 in the primary organs of HB-01-infected hACE2 mice was detected using RT–qPCR. **c**, Virus titres in the lungs were determined on Vero E6 cells. According to a two-tailed unpaired Welch's *t*-test, viral titres in the lungs from HB-01-infected hACE2 mice ($n = 3$) showed a significant increase compared with those in HB-01-infected wild-type mice ($n = 3$) or mock-treated hACE2 mice ($n = 3$) at 1 (**$P = 0.0053$), 3 (**$P = 0.0022$) and 5 (**$P = 0.0081$) dpi. **d**, Virus isolated from the lungs of HB-01-infected hACE2 mice at 3 dpi was observed using electron microscopy. Scale bar, 200 nm. Data are representative of three independent experiments. **e**, The specific IgG against SARS-CoV-2 was detected from the sera of mice (HB-01-infected wild-type ($n = 3$) or hACE2 ($n = 7$) mice) at day 0 and 21 dpi by enzyme-linked immunosorbent assay (ELISA). OD_{450}, optical density at 450 nm. Two-tailed unpaired Student's *t*-test; not significant (NS), $P = 0.2193$; two-tailed unpaired Welch's *t*-test, ***$P = 3.11 \times 10^{-6}$. Data in **a**–**c**, **e** are mean ± s.d.

swallowing. Consistent with the results showing viral loads in the lung, infectious virus was isolated from the lungs of HB-01-infected hACE2 mice at 1, 3 and 5 dpi; the highest virus titres were detected at 3 dpi ($10^{2.44}$ $TCID_{50}$ per 100 µl) (Fig. 1c). We isolated infectious virus using Vero E6 cell culture from the lung, and observed SARS-CoV-2 particles using electron microscopy (Fig. 1d). However, the virus was not isolated from the lungs of HB-01-infected wild-type mice or mock-treated hACE2 mice along the detecting timeline (Fig. 1c), which suggests that human ACE2 is essential for SARS-CoV-2 infection and replication in mice. Moreover, we found specific IgG antibodies against the spike (S) protein of SARS-CoV-2 in the sera of HB-01-infected hACE2 mice at 21 dpi (Fig. 1e).

There were no obviously gross pathological or histopathological changes at 1 dpi in any of the mice. Compared with HB-01-infected wild-type mice or mock-treated hACE2 mice (both of which showed homogeneously pink and slightly deflated lung lobes), HB-01-infected hACE2 mice at 3 dpi displayed gross lesions with focal-to-multifocal dark-red discoloration in some of the lung lobes. The lesions progressed into multifocal-to-coalescent scattered dark-reddish-purple areas and focal palpable nodules throughout the lung lobes at 5 dpi (Fig. 2a). The damaged lungs became swollen and enlarged. Microscopically, the lung tissues from HB-01-infected hACE2 mice at 3 dpi displayed moderate interstitial pneumonia, characterized by thickened alveolar septa accompanied by infiltration of inflammatory cells in 70–80% of the lung tissues, and an accumulation of inflammatory cells in partial alveolar cavities (20–30%). Inflammatory cells—including lymphocytes, macrophages and neutrophils—accumulated in the alveolar interstitium and caused thickening of the alveolar walls. At 5 dpi, the lung progressed into coalescing interstitial pneumonia with diffuse lesions, characterized by more-severe thickened alveolar septa accompanied with infiltration of inflammatory cells, and accumulation of inflammatory cells in more alveolar cavities (40–50%). The thickened alveolar septa were filled with macrophages, lymphocytes and neutrophils (Fig. 2a). A small amount of collagen fibre was observed in the thickened alveolar interstitium in the HB-01-infected hACE2 mice by modified Masson's trichrome stain at 5 dpi (Extended Data Fig. 1a). The bronchiolar epithelial cells showed swelling and degeneration; some of these cells fragmented (Fig. 2a). A few periodic-acid–Schiff-positive-exudation, or denatured and detached, bronchiolar epithelia were occasionally observed in affected bronchioles at 5 dpi (Extended Data Fig. 1b). The alveolar cavities were distended mainly by swollen and degenerative macrophages, lymphocytes and neutrophils (Fig. 2a). To investigate the infiltration of specific inflammatory cells, immunohistochemistry (IHC) was carried out to identify $MAC2^+$ macrophages (Extended Data Fig. 2a), $CD3^+$ T lymphocytes and $CD19^+$ B lymphocytes (Extended Data Fig. 2b). Compared to the lungs of HB-01-infected wild-type mice, more macrophages and T lymphocytes were found in the lungs of HB-01-infected hACE2 mice and their numbers increased along with the prolonged infection time. $MAC2^+$ macrophages were diffusely infiltrated into the alveolar cavities (at 3 dpi) or focally aggregated in the thickened

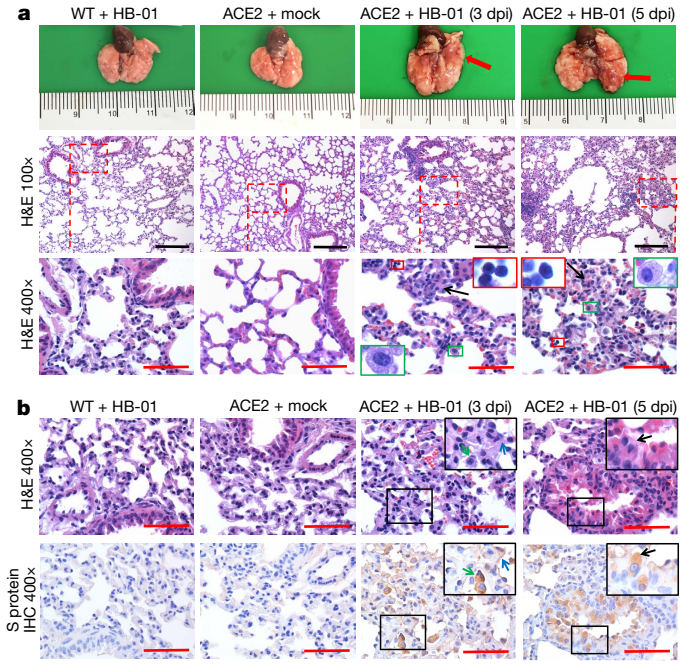

Fig. 2 | Gross pathology, histopathology and IHC of the lungs in hACE2 mice infected with SARS-CoV-2. a, Gross pathology and histopathology of lungs from HB-01-infected wild-type mice (3 dpi), mock-treated hACE2 mice (3 dpi) and HB-01-infected hACE2 mice (3 and 5 dpi). Post-mortem examinations showed focal dark-red lesions (red arrow) throughout the dorsal region of the right middle lobe of the lung at 3 dpi. The lesions progressed into multifocally scattered dark-reddish-purple areas and palpable nodules (red arrow) throughout the right lobe of the lung at 5 dpi. Histopathological observations indicated that moderate interstitial pneumonia with thickened alveolar septa (black arrows) and infiltration of lymphocytes (red frames, 1,000× magnification). The swollen and degenerative mononuclear cells (green frames, 1,000× magnification) are scattered within the alveolar cavities at 3 and 5 dpi. **b**, IHC examination of the lungs of each mouse group. The sequential sections were stained by haematoxylin and eosin (H&E) or IHC. Viral antigens were observed in the mononuclear cells (green arrows), alveolar epithelia (blue arrows) and bronchial epithelial cells that were degenerative and being desquamated (black arrows). The black frames in the top-right corners are a magnification of the region in the respective black box. Scale bars, 100 μm (black), 50 μm (red). Data in **a**, **b** are representative of three independent experiments.

alveolar septa (at 5 dpi) (Extended Data Fig. 2a). $CD3^+$ T lymphocytes were dispersed or (occasionally) aggregated in the alveolar interstitium in HB-01-infected hACE2 mice at 3 and 5 dpi, and some $CD19^+$ B lymphocytes were also observed at 5 dpi (Extended Data Fig. 2b). Perivascular infiltrating inflammatory cells—including lymphocytes, macrophages and neutrophils—were observed multifocally within and adjacent to affected areas of the lungs. In lung lesions, IHC staining of sequential sections revealed that viral antigens were found in macrophages, alveolar epithelia and in bronchial epithelial cells that were degenerative and being desquamated (Fig. 2b). We also observed small amounts of viral antigen in respiratory epithelial cells in areas of the lungs that did not show lesions (data not shown). However, there were no substantial histopathological changes (Extended Data Fig. 3) or viral antigens for SARS-CoV-2 (Extended Data Fig. 4) in the other organs, including myocardium, liver, spleen, kidney, cerebrum, intestine and testis. At 7 dpi, the pneumonia became mild with focal lesion areas (data not shown).

In addition, we demonstrated the colocalization of SARS-CoV-2 S protein (Fig. 3f) and the human ACE2 receptor (Fig. 3g) in alveolar epithelial cells of HB-01-infected hACE2 mice using immunofluorescence, at 3 dpi (Fig. 3h). This phenomenon was not found in mock-treated hACE2 mice (Fig. 3a–d) or HB-01-infected wild-type mice (data not shown), which indicates that SARS-CoV-2—as with SARS-CoV—uses the human ACE2 as a receptor for entry[5].

The speed of the geographical spread of COVID-19 has led to the disease being declared a public health emergency of international concern, with cases reported on multiple continents only weeks after the disease was first reported[6]. Although it has been determined by bioinformatics that the pathogen that causes this epidemic is a novel coronavirus, it is necessary that this is confirmed by animal experiments (following Koch's postulates)[7]. Previous clinical studies have confirmed the isolation of the virus from hosts with the disease and cultivation in host cells[1]. Here we show that, after the experimental infection of hACE2 mice with one of the earliest known isolates of SARS-CoV-2, our mouse model of SARS-CoV-2 infection exhibits viral replication in the lungs characterized by moderate interstitial pneumonia—similar to initial clinical reports of pneumonia caused by SARS-CoV-2[8]. Moreover, we also observed specific antibodies against SARS-CoV-2 and re-isolated the virus from infected mice.

The fatality rate of currently reported cases of COVID-19 is about 2%, which implies that—so far—SARS-CoV-2 does not seem to cause the high fatality rates seen for SARS-CoV (9–11%)[9]; this suggests that

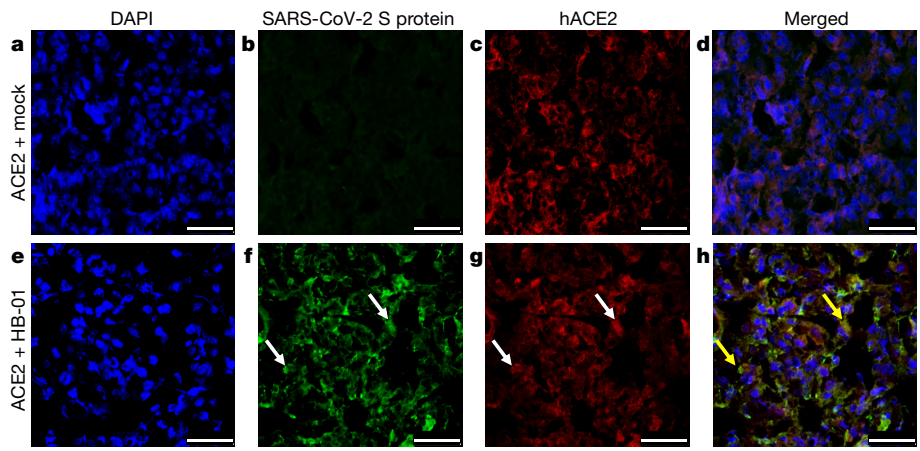

Fig. 3 | Immunofluorescence analysis of viral antigens in the lungs of SARS-CoV-2-infected hACE2 mice at 3 dpi. Colocalization of SARS-CoV-2 S protein and human ACE2 receptor in the lungs of hACE2 mice. The sections were incubated with anti-SARS-CoV-2 S protein antibody, anti-human ACE2 antibody and DAPI. **a**–**d**, Lung sections of mock-treated hACE2 mice. **e**–**h**, Lung sections of HB-01-infected hACE2 mice. White arrows show the viral S protein (**f**) and human ACE2 (**g**); yellow arrows show the merge of viral S protein and human ACE2 (**h**). Scale bars, 25 μm. Data in **a**–**h** are representative of three independent experiments.

there are differences in pathogenicity between the two viruses. In mice, the pathogenicity of SARS-CoV-2 seems mild compared to SARS-CoV; the latter causes extrapulmonary organ damage (including the brain, kidney, intestine, heart and liver) and, furthermore, neurons are susceptible to infection with SARS-CoV—cerebral vasculitis and haemorrhage were observed in SARS-CoV-infected hACE2 mice[10,11]. However, only interstitial pneumonia was observed in SARS-CoV-2-infected hACE2 mice, which implies a disparity in pathogenicity between the two coronaviruses.

Our results demonstrate the pathogenicity of SARS-CoV-2 in mice, which—together with previous clinical studies[1]—completely satisfies Koch's postulates[7] and confirms that SARS-CoV-2 is the pathogen responsible for COVID-19. Our mouse model of SARS-CoV-2 infection will be valuable for evaluating antiviral therapeutic agents and vaccines, as well as understanding the pathogenesis of this disease.

Note added in proof: In the version of this paper that was originally published online, Fig. 2a contained a duplication. In the version of the figure that was originally published, tissue sections from a WT + HB-01 sample were shown instead of tissue sections from ACE2 + mock. The originally published figure can be found here as Supplementary Fig. 1.

Online content

Any methods, additional references, Nature Research reporting summaries, source data, extended data, supplementary information, acknowledgements, peer review information; details of author contributions and competing interests; and statements of data and code availability are available at https://doi.org/10.1038/s41586-020-2312-y.

1. Zhu, N. et al. A novel coronavirus from patients with pneumonia in China, 2019. *N. Engl. J. Med.* **382**, 727–733 (2020).
2. Kuba, K. et al. A crucial role of angiotensin converting enzyme 2 (ACE2) in SARS coronavirus-induced lung injury. *Nat. Med.* **11**, 875–879 (2005).
3. Ren, L. L. et al. Identification of a novel coronavirus causing severe pneumonia in human: a descriptive study. *Chin. Med. J. (Engl.)* **133**, 1015–1024 (2020).
4. China National Health Commission. *Update on the Novel Coronavirus Pneumonia Outbreak (Jan 24, 2020)*. http://www.nhc.gov.cn/yjb/s7860/202002/84faf71e096446fdb1ae44939ba5c528.shtml (China National Health Commission, 2020).
5. Xu, X. et al. Evolution of the novel coronavirus from the ongoing Wuhan outbreak and modeling of its spike protein for risk of human transmission. *Sci. China Life Sci.* **63**, 457–460 (2020).
6. Chan, J. F. et al. A familial cluster of pneumonia associated with the 2019 novel coronavirus indicating person-to-person transmission: a study of a family cluster. *Lancet* **395**, 514–523 (2020).
7. Rivers, T. M. Viruses and Koch's postulates. *J. Bacteriol.* **33**, 1–12 (1937).
8. Huang, C. et al. Clinical features of patients infected with 2019 novel coronavirus in Wuhan, China. *Lancet* **395**, 497–506 (2020).
9. de Wit, E., van Doremalen, N., Falzarano, D. & Munster, V. J. SARS and MERS: recent insights into emerging coronaviruses. *Nat. Rev. Microbiol.* **14**, 523–534 (2016).
10. Yang, X. H. et al. Mice transgenic for human angiotensin-converting enzyme 2 provide a model for SARS coronavirus infection. *Comp. Med.* **57**, 450–459 (2007).
11. Netland, J., Meyerholz, D. K., Moore, S., Cassell, M. & Perlman, S. Severe acute respiratory syndrome coronavirus infection causes neuronal death in the absence of encephalitis in mice transgenic for human ACE2. *J. Virol.* **82**, 7264–7275 (2008).

Methods

No statistical methods were used to predetermine sample size. The experiments were not randomized and investigators were not blinded to allocation during experiments and outcome assessment.

Ethics statement

Mouse studies were performed in an animal biosafety level 3 (ABSL3) facility using HEPA-filtered isolators. All procedures in this study involving mice were reviewed and approved by the Institutional Animal Care and Use Committee of the Institute of Laboratory Animal Science, Peking Union Medical College (BLL20001). All of the experiments complied with all relevant ethical regulations.

Viruses and cells

The SARS-CoV-2 strain HB-01 was provided by W. Tan[1]. The complete genome for this SARS-CoV-2 has been submitted to GISAID (identifier: BetaCoV/Wuhan/IVDC-HB-01/2020|EPI_ISL_402119), and deposited in the China National Microbiological Data Center (accession number NMDC10013001 and genome accession number MDC60013002-01). Seed SARS-CoV-2 stocks and virus isolation studies were performed in Vero cells, which are maintained in Dulbecco's modified Eagle's medium (DMEM) (Invitrogen) supplemented with 10% fetal bovine serum (FBS), 100 IU/ml penicillin, and 100 μg/ml streptomycin, and incubated at 37 °C, 5% CO_2. For infected mice, lung homogenates were used for virus titration tests using endpoint titration in Vero E6 cells. Virus titres of the supernatant were determined using a standard $TCID_{50}$ assay.

Mouse experiments

For the mouse experiments, specific-pathogen-free, 6–11-month-old male and female hACE2 mice were obtained from the Institute of Laboratory Animal Science, Peking Union Medical College. Transgenic mice were generated by microinjection of the mouse *Ace2* promoter driving the human *ACE2* coding sequence into the pronuclei of fertilized ova from ICR mice, and then human ACE2 integrated was identified by PCR as previous described[10]; the human ACE2 mainly expressed in the lungs, heart, kidneys and intestines of transgenic mice. After being intraperitoneally anaesthetized by 2.5% avertin with 0.02 ml/g body weight, the hACE2 or wild-type (ICR) mice were inoculated intranasally with SARS-CoV-2 stock virus at a dosage of 10^5 $TCID_{50}$, and hACE2 mice intranasally inoculated with an equal volume of PBS were used as a mock-infection control. The infected mice were continuously observed to record body weight, clinical symptoms, responses to external stimuli and death. Mice were dissected at 1, 3, 5 and 7 dpi to collect different tissues to screen virus replication and histopathological changes.

Preparation of homogenate supernatant

Tissues homogenates (1 g/ml) were prepared by homogenizing perfused tissues using an electric homogenizer for 2 min 30 s in DMEM. The homogenates were centrifuged at 3,000 rpm for 10 min at 4 °C. The supernatant was collected and stored at −80 °C for viral titre and viral load detection.

RNA extraction and RT–qPCR

Total RNA was extracted from tissues homogenates of organs using the RNeasy Mini Kit (Qiagen), and reverse transcription was performed using the PrimerScript RT Reagent Kit (TaKaRa) following the manufacturers' instructions. RT–qPCR reactions were performed using the PowerUp SYBG Green Master Mix Kit (Applied Biosystems), in which samples were processed in duplicate using the following cycling protocol: 50 °C for 2 min, 95 °C for 2 min, followed by 40 cycles at 95 °C for 15 s and 60 °C for 30 s, and then 95 °C for 15 s, 60 °C for 1 min, 95 °C for 45 s. The primer sequences used for RT–qPCR are targeted against the envelope (*E*) gene of SARS-CoV-2 and are as follows: forward: 5′-TCGTTTCGGAAGAGACAGGT-3′, reverse: 5′-GCGCAGTAAGGATGGCTAGT-3′. The PCR products were verified by sequencing using the dideoxy method on an ABI 3730 DNA sequencer (Applied Biosystems). During the sequencing process, amplification was performed using specific primers. The sequences for this process are available upon request to the corresponding author. The sequencing reads obtained were linked using DNAMAN, and the results were compared using the Megalign module in the DNAStar software package. The SYBR green real-time PCR standard curve was generated by serial tenfold dilutions of recombinant plasmid with a known copy number (from 1.47×10^9 to 1.47×10^1 copies per μl). These dilutions were tested and used as quantification standards to construct the standard curve by plotting the plasmid copy number against the corresponding threshold cycle values (C_t). Results were expressed as $\log_{10}$-transformed numbers of genome equivalent copies per ml of sample.

ELISA method

The specific IgG against SARS-CoV-2 from HB-01-infected hACE2 and wild-type mice was determined by ELISA. Ninety-six-well plates were coated with the Spike 1 (S1) protein of SARS-CoV-2 (0.1 μg/100 μl, Sino Biological, 40591-V08H), the tested sera were diluted at 1:100 and added to each well, and 3 multiple wells were set for each sample, and then incubated at 37 °C for 30 min, followed by goat anti-mouse secondary antibodies conjugated with HRP (ZB-2305, zhongshan,1:10,000 dilution), and incubated at room temperature for 30 min. The reaction was developed by TMB substrate and the optical densities at 450 nm were determined (Metertech960 enzyme marker with 450 nm wavelength).

Laboratory preparation of the antibody of SARS-CoV-2 S1 protein

Mice were immunized with purified SARS-CoV-2 S1 protein (Sino biological) and splenocytes of hyper-immunized mice were fused with myeloma cells. Positive clones were selected by ELISA using SARS-CoV-2 S1 protein (Extended Data Fig. 5). The cell supernatant of 7D2 clone, which binds to the SARS-CoV-2 S1 protein, was collected for immunofluorescence analysis.

Pathological examination

Autopsies were performed in an animal biosafety level 3 (ABSL3) laboratory. Major organs were grossly examined and then fixed in 10% buffered formalin solution, and paraffin sections (3–4 μm in thickness) were prepared routinely. Haematoxylin and eosin, periodic acid–Schiff and modified Masson's trichrome stains were used to identify histopathological changes in all of the organs. The histopathology of the lung tissue was observed by light microscopy.

IHC

The organs were fixed in 10% buffered formalin solution, and paraffin sections (3–4 μm in thickness) were prepared routinely. Sections were treated with an antigen retrieval kit (Boster, AR0022) for 1 min at 37 °C and quenched for endogenous peroxidases in 3% H_2O_2 in methanol for 10 min. After blocking in 1% normal goat serum, the sections were incubated with 7D2 monoclonal antibody (laboratory preparation) at 4 °C overnight, followed by HRP-labelled goat anti-mouse IgG secondary antibody (Beijing ZSGB Biotechnology, ZDR-5307). Alternatively, the sections were stained with rat IgG2a antibody (Abcam, ab18450, RTK2758), MAC2 antibody (Cedarlane Laboratories, CL8942AP), CD3 antibody (Dako, A0452) or CD19 antibody (Cell Signaling Technology, 3574) at 4 °C overnight. Subsequently, the sections were incubated with goat anti-rat IgG secondary antibody (HRP) (Beijing ZSGB Biotechnology, PV9004) or goat anti-rabbit IgG secondary antibody (HRP) (Beijing ZSGB Biotechnology, PV9001) for 60 min, and visualized by 3,30-diaminobenzidine tetrahydrochloride (DAB). The slices were counterstained with haematoxylin, dehydrated and mounted on a slide and viewed under an Olympus microscope. The sections from HB-01-infected wild-type mice, mock-treated hACE2 mice or

HB-01-infected hACE2 mice were directly incubated with HRP-labelled goat anti-rat/mouse/rabbit IgG and used as the negative control for MAC2, CD19, CD3 or viral antigen staining. Rat IgG2a antibody was used as isotype control for MAC2 staining. For the expression of viral antigen, the sections from HB-01-infected wild-type mice or mock-treated hACE2 mice incubated with anti-S protein antibody was also used as a negative control.

Confocal microscopy

For analysis of the colocalization of viruses and the human ACE2 receptor, the lung tissue sections were washed twice with PBS, fixed by Immunol staining fix solution (P0098, Beyotime Biotechnology), blocked for 1 h at room temperature by Immunol staining blocking buffer (P0102, Beyotime Biotechnology) and then incubated overnight at 4 °C with the appropriate primary and secondary antibodies. The nuclei were stained with DAPI. Anti-S protein antibody (mouse monoclonal 7D2, laboratory preparation, 1:200) and anti-hACE2 antibody (rabbit polyclonal, ab15348, Abcam, 1:200) were used as the primary antibodies. The sections were washed with PBS and incubated with secondary antibodies conjugated with FITC (goat anti-mouse, ZF-0312, Beijing ZSGB Biotechnology, 1:200) and TRITC (goat anti rabbit, ZF-0317, Beijing ZSGB Biotechnology, 1:200), dried at room temperature and observed via fluorescence microscopy. The sections from mock-treated or HB-01-infected hACE2 mice were directly incubated with FITC-conjugated goat anti-mouse IgG or TRITC-conjugated goat anti-rabbit IgG and used as the negative control. For the expression of human ACE2, the sections from wild-type mice stained with anti-ACE2 antibody were used as the negative control, and the stable cell line expressing human ACE2 was used as the positive control. For the viral antigen, the sections from mock-treated hACE2 mice incubated with anti-S protein antibody were used as the negative control.

Transmission electron microscopy

Supernatant from Vero E6 cell cultures that showed cytopathic effects was collected, inactivated with 2% paraformaldehyde for at least 2 h, and ultracentrifuged to sediment virus particles. The enriched supernatant was negatively stained on film-coated grids for examination. The negative stained grids were observed under transmission electron microscopy.

Statistical analysis

All data were analysed with GraphPad Prism 8.0 software. Statistically significant differences were determined using unpaired *t*-tests, Student's *t*-tests, Welch's *t*-tests or Mann–Whitney *U*-tests, as applicable and according to test requirements. A two-sided P value < 0.05 was considered statistically significant. $^{*}P < 0.05$, $^{**}P < 0.01$, $^{***}P < 0.001$. No statistical methods were used to predetermine sample size. The experiments were not randomized and the investigators were not blinded to allocation during experiments and outcome assessment.

Reporting summary

Further information on research design is available in the Nature Research Reporting Summary linked to this paper.

Data availability

All raw data are available from the corresponding authors on reasonable request. Source data are provided with this paper.

Acknowledgements We thank G. F. Gao for his advice and coordination on this work; H. Deng, X. Yang and L. Zhang for providing the hACE2 mice as a gift; and G. Wong for helping us to proofread the manuscript. This work was supported by National Research and Development Project of China (2020YFC0841100), Fundamental Research Funds for CAMS of China (2020HY320001), National Key Research and Development Project of China (2016YFD0500304), CAMS initiative for Innovative Medicine of China (2016-I2M-2-006) and National Mega projects of China for Major Infectious Diseases (2017ZX10304402, 2018ZX10301403).

Author contributions C.Q. and G. Wu conceptualized the study. L.B., W.D., B.H., H.G. and J.L. constructed the methodology. L.B., W.D., B.H., H.G., J.L., L.R., Q.W., P.Y., Y. Xiao, F.Q., Y.Q., F.L., Q.L., W.W., J.X., S.G., M.L., G. Wang, S.W., Z.S., Li Zhao, P.L., Linna Zhao, F.Y., H.W., W. Zhou, N.Z., W. Zhen, H.Y., X.Z., L.G., L.C., C.W., Y.W., X.W., Y. Xu, Q.S., H.L., F.Z., C.M., L.Y., M.Y., J.H., W.X., W.T., X.P. and Q.J. performed the investigations. L.B., J.L., J.X. and Z.S. wrote the original draft, which was reviewed and edited by C.Q. and G. Wu. Funding was acquired by C.Q. and L.B. Resources were provided by C.Q. C.Q. and G. Wu supervised the project.

Competing interests The authors declare no competing interests.

Additional information
Supplementary information is available for this paper at https://doi.org/10.1038/s41586-020-2312-y.
Correspondence and requests for materials should be addressed to G. Wu or C.Q.
Peer review information Peer reviewer reports are available.
Reprints and permissions information is available at http://www.nature.com/reprints.

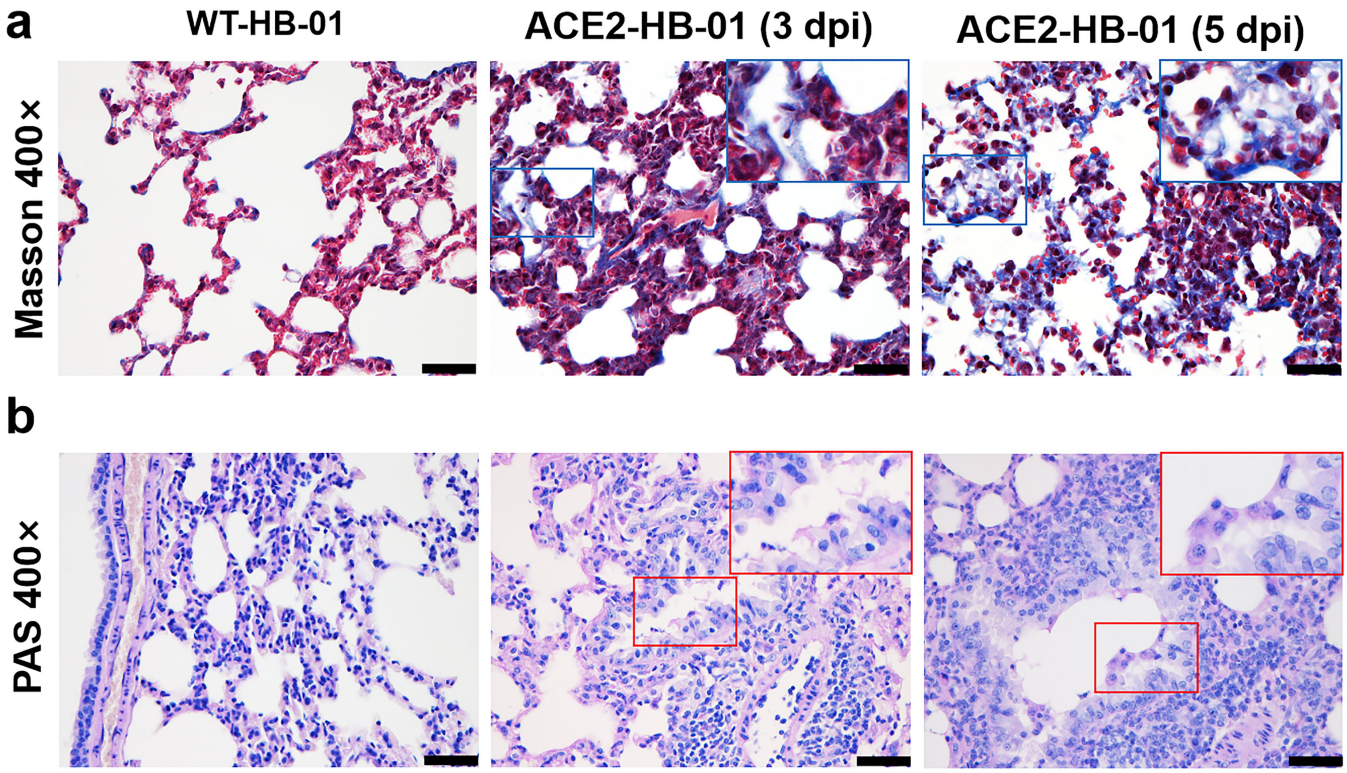

Extended Data Fig. 1 | Stains of the lungs in HB-01-infected wild-type and hACE2 mice at 3 and 5 dpi. a, Modified Masson's trichrome stain of the lung. Compared to the HB-01-infected wild-type mice, increased collagen fibres (blue-stained fibres) in the thickened alveolar interstitium were observed in the HB-01-infected hACE2 mice at 3 and 5 dpi. Blue frames in the top-right corners are magnifications of the region in the corresponding blue box. **b**, Periodic acid–Schiff (PAS) stain of the respiratory epithelium in bronchioles. A small amount of mucus accumulated on the surface of bronchial epithelial cells. Red frames in the top-right corners are magnifications of the region in the corresponding red box. Scale bars, 40 μm. Data in **a**, **b** are representative of three independent experiments.

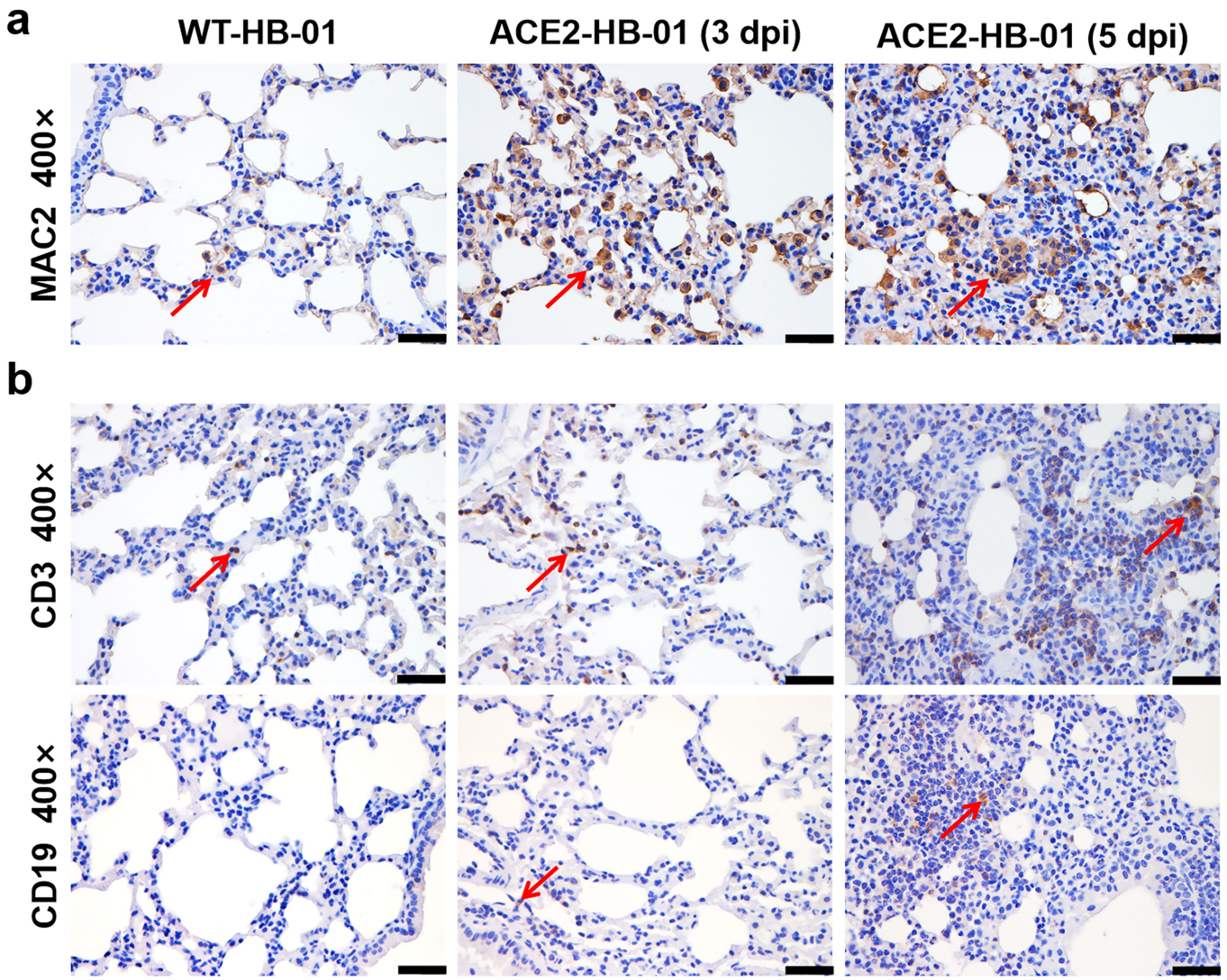

Extended Data Fig. 2 | IHC was carried out to identify MAC2$^+$ macrophages, CD3$^+$ T lymphocytes and CD19$^+$ B lymphocytes. a, Diffuse infiltration of macrophages (red arrow) in the expanded alveolar septa in HB-01-infected hACE2 mice at 3 and 5 dpi. **b**, Many T lymphocytes (red arrow) infiltrated the thickened alveolar septa in the first row of **b** at 5 dpi in the HB-01-infected hACE2 mice. A few B lymphocytes (red arrow) were observed in the HB-01-infected hACE2 mice. Scale bars, 40 μm. Data in **a**, **b** are representative of three independent experiments.

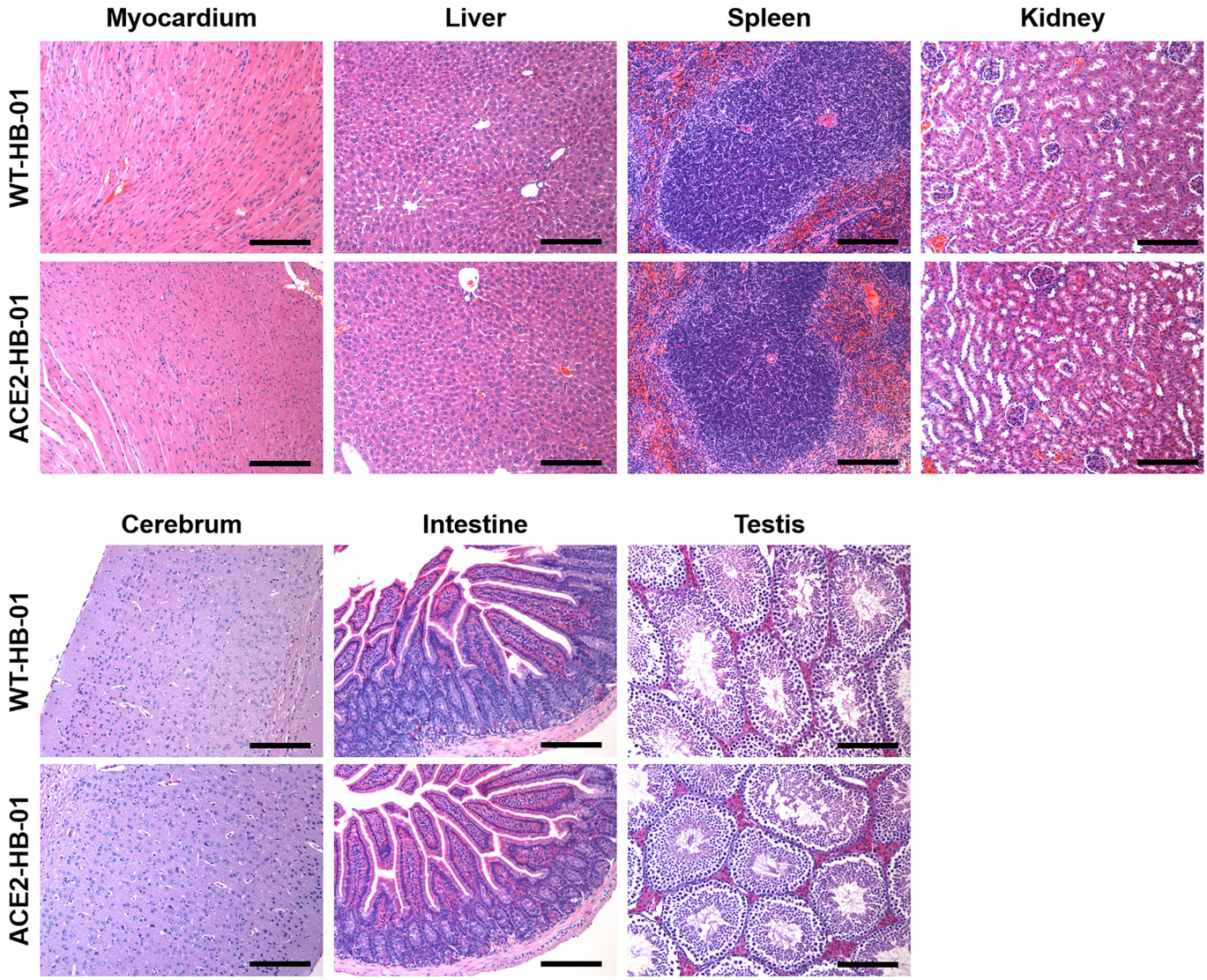

Extended Data Fig. 3 | Histopathological observations of the organs in HB-01-infected wild-type and hACE2 mice. There were no substantial histopathological changes in the organs (including myocardium, liver, spleen, kidney, cerebrum, intestine and testis) in HB-01-infected hACE2 mice compared with HB-01-infected wild-type mice. Scale bars, 100 μm. Data are representative of three independent experiments.

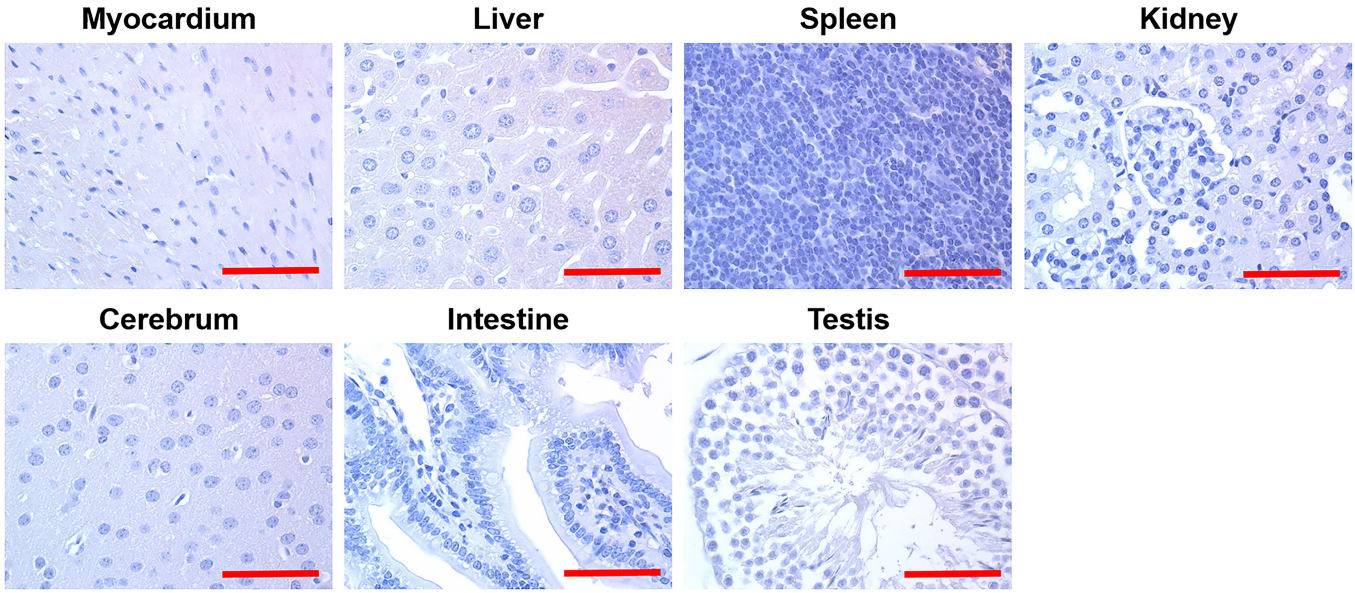

Extended Data Fig. 4 | IHC observations of the organs in HB-01-infected hACE2 mice. There were no SARS-CoV-2 antigens in the organs (including myocardium, liver, spleen, kidney, cerebrum, intestine and testis). Scale bars, 50 μm. Data are representative of three independent experiments.

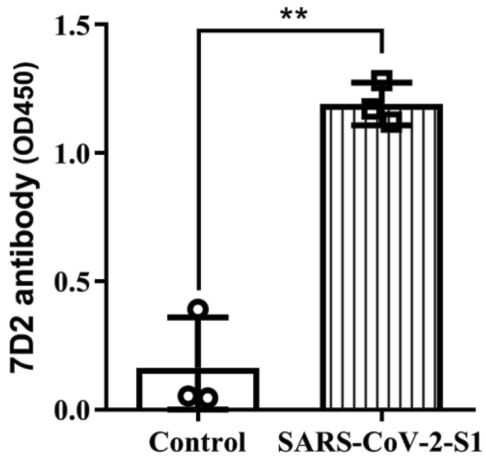

Extended Data Fig. 5 | Identification of 7D2 antibody against SARS-CoV-2 S1 protein. The plate coated with 0.2 μg SARS-CoV-2 S1 protein was incubated with 7D2 antibody as primary antibody (1:200), and detected using HRP-conjugated goat anti-mouse secondary antibody. The titre of antibody was determined using ELISA. Data are mean ± s.d. Significant differences are indicated with asterisks ($n = 3$, two-tailed unpaired Student's t-test, $^{**}P = 0.0011$).

nature research

Corresponding author(s): Chuan Qin

Last updated by author(s): Mar 20, 2020

Reporting Summary

Nature Research wishes to improve the reproducibility of the work that we publish. This form provides structure for consistency and transparency in reporting. For further information on Nature Research policies, see Authors & Referees and the Editorial Policy Checklist.

Statistics

For all statistical analyses, confirm that the following items are present in the figure legend, table legend, main text, or Methods section.

n/a	Confirmed	
☐	☒	The exact sample size (*n*) for each experimental group/condition, given as a discrete number and unit of measurement
☐	☒	A statement on whether measurements were taken from distinct samples or whether the same sample was measured repeatedly
☐	☒	The statistical test(s) used AND whether they are one- or two-sided *Only common tests should be described solely by name; describe more complex techniques in the Methods section.*
☐	☒	A description of all covariates tested
☐	☒	A description of any assumptions or corrections, such as tests of normality and adjustment for multiple comparisons
☐	☒	A full description of the statistical parameters including central tendency (e.g. means) or other basic estimates (e.g. regression coefficient) AND variation (e.g. standard deviation) or associated estimates of uncertainty (e.g. confidence intervals)
☐	☒	For null hypothesis testing, the test statistic (e.g. *F*, *t*, *r*) with confidence intervals, effect sizes, degrees of freedom and *P* value noted *Give P values as exact values whenever suitable.*
☒	☐	For Bayesian analysis, information on the choice of priors and Markov chain Monte Carlo settings
☒	☐	For hierarchical and complex designs, identification of the appropriate level for tests and full reporting of outcomes
☒	☐	Estimates of effect sizes (e.g. Cohen's *d*, Pearson's *r*), indicating how they were calculated

Our web collection on statistics for biologists contains articles on many of the points above.

Software and code

Policy information about availability of computer code

Data collection	All data were collected with GraphPad Prism 8.0 software (GraphPad Software Inc., San Diego, CA)
Data analysis	All data analysis were performed with GraphPad Prism 8.0 software (GraphPad Software Inc., San Diego, CA)

For manuscripts utilizing custom algorithms or software that are central to the research but not yet described in published literature, software must be made available to editors/reviewers. We strongly encourage code deposition in a community repository (e.g. GitHub). See the Nature Research guidelines for submitting code & software for further information.

Data

Policy information about availability of data

All manuscripts must include a data availability statement. This statement should provide the following information, where applicable:

- Accession codes, unique identifiers, or web links for publicly available datasets
- A list of figures that have associated raw data
- A description of any restrictions on data availability

The complete genome for this SARS-CoV-2 was submitted to GISAID (BetaCoV/Wuhan/IVDC-HB-01/2020|EPI_ISL_402119), and deposited in the Novel Coronavirus National Science and Technology Resource Service System (http://nmdc.cn/nCoV, accession number NMDC10013001 and genome accession numbers MDC60013002-01). All data are available without any restrictions.

Field-specific reporting

Please select the one below that is the best fit for your research. If you are not sure, read the appropriate sections before making your selection.

☒ Life sciences ☐ Behavioural & social sciences ☐ Ecological, evolutionary & environmental sciences

For a reference copy of the document with all sections, see nature.com/documents/nr-reporting-summary-flat.pdf

Life sciences study design

All studies must disclose on these points even when the disclosure is negative.

Sample size	No statistical methods were used to predetermine sample size. For the animal study, there are three groups investigated, including hACE2 transgenic mice group (ACE2-HB-01, n=19) and wild type ICR mice group (WT-HB-01, n=15) with SARS-CoV-2 infection, and hACE2 transgenic mice group without infection (ACE2-Mock, n=15). The numbers of mice in each group meet the requirement for statistical analysis (at least 3 for each group per time-point), which is sufficient given the excellent technical reproducibility.
Data exclusions	No data were excluded from the analyses.
Replication	Nineteen or fifteen mice were included for each group, and the results were compared with the same trend. As for the viral loads, viral titers, IHC, IF, HE stain, Masson stain and PAS stain experiments, 3 mice for each group (at each detecting time-point) were tested, and some of them were repeated twice separately by two technicians. All attempts at replication were successful.
Randomization	For the animal study, we have designed a time-dependent pathological experiments in 12 WT-HB-01 mice, 12 ACE2-mock and 12 ACE2-HB-01 for euthanasia. These 12 mice per group were randomly divided in to the four groups to undergo four time-point measurements (1 dpi, 3 dpi, 5 dpi and 7 dpi). The tests were also randomly selected from all samples. The pictures were representatively shown.
Blinding	During the study, all mice and all samples were coded. The technicians did not know which animal or sample is hACE2 transgenic or wild type, with or without virus infection.

Behavioural & social sciences study design

All studies must disclose on these points even when the disclosure is negative.

Study description	*Briefly describe the study type including whether data are quantitative, qualitative, or mixed-methods (e.g. qualitative cross-sectional, quantitative experimental, mixed-methods case study).*
Research sample	*State the research sample (e.g. Harvard university undergraduates, villagers in rural India) and provide relevant demographic information (e.g. age, sex) and indicate whether the sample is representative. Provide a rationale for the study sample chosen. For studies involving existing datasets, please describe the dataset and source.*
Sampling strategy	*Describe the sampling procedure (e.g. random, snowball, stratified, convenience). Describe the statistical methods that were used to predetermine sample size OR if no sample-size calculation was performed, describe how sample sizes were chosen and provide a rationale for why these sample sizes are sufficient. For qualitative data, please indicate whether data saturation was considered, and what criteria were used to decide that no further sampling was needed.*
Data collection	*Provide details about the data collection procedure, including the instruments or devices used to record the data (e.g. pen and paper, computer, eye tracker, video or audio equipment) whether anyone was present besides the participant(s) and the researcher, and whether the researcher was blind to experimental condition and/or the study hypothesis during data collection.*
Timing	*Indicate the start and stop dates of data collection. If there is a gap between collection periods, state the dates for each sample cohort.*
Data exclusions	*If no data were excluded from the analyses, state so OR if data were excluded, provide the exact number of exclusions and the rationale behind them, indicating whether exclusion criteria were pre-established.*
Non-participation	*State how many participants dropped out/declined participation and the reason(s) given OR provide response rate OR state that no participants dropped out/declined participation.*
Randomization	*If participants were not allocated into experimental groups, state so OR describe how participants were allocated to groups, and if allocation was not random, describe how covariates were controlled.*

Ecological, evolutionary & environmental sciences study design

All studies must disclose on these points even when the disclosure is negative.

Study description	*Briefly describe the study. For quantitative data include treatment factors and interactions, design structure (e.g. factorial, nested, hierarchical), nature and number of experimental units and replicates.*
Research sample	*Describe the research sample (e.g. a group of tagged Passer domesticus, all Stenocereus thurberi within Organ Pipe Cactus National Monument), and provide a rationale for the sample choice. When relevant, describe the organism taxa, source, sex, age range and any manipulations. State what population the sample is meant to represent when applicable. For studies involving existing datasets, describe the data and its source.*
Sampling strategy	*Note the sampling procedure. Describe the statistical methods that were used to predetermine sample size OR if no sample-size calculation was performed, describe how sample sizes were chosen and provide a rationale for why these sample sizes are sufficient.*
Data collection	*Describe the data collection procedure, including who recorded the data and how.*
Timing and spatial scale	*Indicate the start and stop dates of data collection, noting the frequency and periodicity of sampling and providing a rationale for these choices. If there is a gap between collection periods, state the dates for each sample cohort. Specify the spatial scale from which the data are taken*
Data exclusions	*If no data were excluded from the analyses, state so OR if data were excluded, describe the exclusions and the rationale behind them, indicating whether exclusion criteria were pre-established.*
Reproducibility	*Describe the measures taken to verify the reproducibility of experimental findings. For each experiment, note whether any attempts to repeat the experiment failed OR state that all attempts to repeat the experiment were successful.*
Randomization	*Describe how samples/organisms/participants were allocated into groups. If allocation was not random, describe how covariates were controlled. If this is not relevant to your study, explain why.*
Blinding	*Describe the extent of blinding used during data acquisition and analysis. If blinding was not possible, describe why OR explain why blinding was not relevant to your study.*

Did the study involve field work? ☐ Yes ☐ No

Field work, collection and transport

Field conditions	*Describe the study conditions for field work, providing relevant parameters (e.g. temperature, rainfall).*
Location	*State the location of the sampling or experiment, providing relevant parameters (e.g. latitude and longitude, elevation, water depth).*
Access and import/export	*Describe the efforts you have made to access habitats and to collect and import/export your samples in a responsible manner and in compliance with local, national and international laws, noting any permits that were obtained (give the name of the issuing authority, the date of issue, and any identifying information).*
Disturbance	*Describe any disturbance caused by the study and how it was minimized.*

Reporting for specific materials, systems and methods

We require information from authors about some types of materials, experimental systems and methods used in many studies. Here, indicate whether each material, system or method listed is relevant to your study. If you are not sure if a list item applies to your research, read the appropriate section before selecting a response.

Materials & experimental systems

n/a	Involved in the study
☐	☒ Antibodies
☐	☒ Eukaryotic cell lines
☒	☐ Palaeontology
☐	☒ Animals and other organisms
☒	☐ Human research participants
☒	☐ Clinical data

Methods

n/a	Involved in the study
☒	☐ ChIP-seq
☒	☐ Flow cytometry
☒	☐ MRI-based neuroimaging

Antibodies

Antibodies used

7D2 antibody for anti-SARS-CoV-2 S protein (mouse antibody, laboratory preparation, Supplementary Figure 5,1:200), rat lgG2a antibody (rat antibody, ab18450, Abcam, RTK2758, Low endotoxin, Azide Free,1:1000) , anti-ACE2 antibody (rabbit antibody, Abcam, ab15348, 1:500) , anti-MAC2 antibody (rat antibody, Cedarlane Laboratories, CL8942AP, 1:1000) , anti-CD3 antibody (rabbit antibody, Dako, A0452,1:100), anti-CD19 antibody (rabbit antibody, Cell Signaling Technology, 3574,1:50) , goat anti rabbit lgG conjugated TRITC (goat anti rabbit, ZF-0317, Beijing ZSGB Biotechnology,1:200), goat anti-mouse lgG conjugated FITC, (goat anti-mouse, ZF-0312, Beijing ZSGB Biotechnology,1:200), goat-anti rat lgG conjugated HRP (goat anti-mouse, ZF-0312, Beijing ZSGB Biotechnology,1:200), goat-anti mouse lgG conjugated HRP (ZDR-5307, Beijing ZSGB Biotechnology,1:200), goat-anti rabbitt lgG conjugated HRP (PV9001, Beijing ZSGB Biotechnology,1:200).

Validation

7D2 antibody for anti-SARS-CoV-2 S protein (mouse antibody, laboratory preparation, Supplementary Figure 5,1:200)

Anti-ACE2 antibody (rabbit antibody, Abcam, ab15348, 1:500)
https://www.abcam.cn/ace2-antibody-ab15348.html

Anti-MAC2 antibody (rat antibody, Cedarlane Laboratories, CL8942AP, 1:1000)
https://www.cedarlanelabs.com/products/detail/cl8942ap?lob=AllProducts

Rat lgG2a antibody (rat antibody, ab18450, Abcam, RTK2758, Low endotoxin, Azide Free,1:1000)
https://www.abcam.cn/rat-igg2a-kappa-monoclonal-rtk2758-isotype-control-low-endotoxin-azide-free-ab18450.html

Anti-CD3 antibody (rabbit antibody, Dako, A0452,1:100)
https://www.agilent.com/cs/library/packageinsert/public/P05193CN_02%20A0452.pdf

Anti-CD19 antibody (rabbit antibody, Cell Signaling Technology, 3574,1:50)
https://www.cst-c.com.cn/products/primary-antibodies/cd19-antibody/3574

Secondary antibodies conjugated TRITC (goat anti rabbit, ZF-0317, Beijing ZSGB Biotechnology,1:200)
http://www.zsbio.com/product/ZF-0317

Secondary antibodies conjugated FITC (goat anti-mouse, ZF-0312, Beijing ZSGB Biotechnology,1:200)
http://www.zsbio.com/product/ZF-0312

Goat anti-rat lgG secondary antibody conjugated HRP (PV9004, Beijing ZSGB Biotechnology,1:200)
http://www.zsbio.com/product/PV-9004

Goat anti-mouse lgG secondary antibody conjugated HRP (ZDR-5307, Beijing ZSGB Biotechnology,1:200)
http://www.zsbio.com/product/ZDR-5307

Goat anti-rabbit lgG secondary antibody conjugated HRP (PV9001, Beijing ZSGB Biotechnology,1:200)
http://www.zsbio.com/product/PV-9001

Eukaryotic cell lines

Policy information about cell lines

Cell line source(s)	Vero E6 cells were obtained from ATCC (CRL-1586).
Authentication	To follow the protocol provided by ATCC. None of the cell lines have been authenticated.
Mycoplasma contamination	The cell line tested negative for mycoplasma contamination.
Commonly misidentified lines (See ICLAC register)	There is no commonly misidentified cell lines used in this study.

Palaeontology

Specimen provenance	*Provide provenance information for specimens and describe permits that were obtained for the work (including the name of the issuing authority, the date of issue, and any identifying information).*
Specimen deposition	*Indicate where the specimens have been deposited to permit free access by other researchers.*
Dating methods	*If new dates are provided, describe how they were obtained (e.g. collection, storage, sample pretreatment and measurement), where they were obtained (i.e. lab name), the calibration program and the protocol for quality assurance OR state that no new dates are provided.*

☐ Tick this box to confirm that the raw and calibrated dates are available in the paper or in Supplementary Information.

Animals and other organisms

Policy information about studies involving animals; ARRIVE guidelines recommended for reporting animal research

Laboratory animals	Male and female transgenic hACE2 mice (specific pathogen-free, 6-11-month-old) were obtained from the Institute of Laboratory Animal Science, Peking Union Medical College, China. Transgenic mice were generated by microinjection of the cytomegalovirus promoter driving the human ACE2 coding sequence into Institute of Cancer Research (ICR) mice, the presence of human ACE2 was confirmed in the mice used by PCR.
Wild animals	The study did not involve wild animals.
Field-collected samples	The study did not involve samples collected from the field.
Ethics oversight	All procedures in this study involving animals were reviewed and approved by the Institutional Animal Care and Use Committee of the Institute of Laboratory Animal Science, Peking Union Medical College (BLL20001).

Note that full information on the approval of the study protocol must also be provided in the manuscript.

Human research participants

Policy information about studies involving human research participants

Population characteristics	*Describe the covariate-relevant population characteristics of the human research participants (e.g. age, gender, genotypic information, past and current diagnosis and treatment categories). If you filled out the behavioural & social sciences study design questions and have nothing to add here, write "See above."*
Recruitment	*Describe how participants were recruited. Outline any potential self-selection bias or other biases that may be present and how these are likely to impact results.*
Ethics oversight	*Identify the organization(s) that approved the study protocol.*

Note that full information on the approval of the study protocol must also be provided in the manuscript.

Clinical data

Policy information about clinical studies

All manuscripts should comply with the ICMJE guidelines for publication of clinical research and a completed CONSORT checklist must be included with all submissions.

Clinical trial registration	*Provide the trial registration number from ClinicalTrials.gov or an equivalent agency.*
Study protocol	*Note where the full trial protocol can be accessed OR if not available, explain why.*
Data collection	*Describe the settings and locales of data collection, noting the time periods of recruitment and data collection.*
Outcomes	*Describe how you pre-defined primary and secondary outcome measures and how you assessed these measures.*

ChIP-seq

Data deposition

☐ Confirm that both raw and final processed data have been deposited in a public database such as GEO.

☐ Confirm that you have deposited or provided access to graph files (e.g. BED files) for the called peaks.

Data access links *May remain private before publication.*	*For "Initial submission" or "Revised version" documents, provide reviewer access links. For your "Final submission" document, provide a link to the deposited data.*
Files in database submission	*Provide a list of all files available in the database submission.*
Genome browser session (e.g. UCSC)	*Provide a link to an anonymized genome browser session for "Initial submission" and "Revised version" documents only, to enable peer review. Write "no longer applicable" for "Final submission" documents.*

Methodology

Replicates	*Describe the experimental replicates, specifying number, type and replicate agreement.*
Sequencing depth	*Describe the sequencing depth for each experiment, providing the total number of reads, uniquely mapped reads, length of reads and whether they were paired- or single-end.*
Antibodies	*Describe the antibodies used for the ChIP-seq experiments; as applicable, provide supplier name, catalog number, clone*

Antibodies	*name, and lot number.*
Peak calling parameters	*Specify the command line program and parameters used for read mapping and peak calling, including the ChIP, control and index files used.*
Data quality	*Describe the methods used to ensure data quality in full detail, including how many peaks are at FDR 5% and above 5-fold enrichment.*
Software	*Describe the software used to collect and analyze the ChIP-seq data. For custom code that has been deposited into a community repository, provide accession details.*

Flow Cytometry

Plots

Confirm that:

☐ The axis labels state the marker and fluorochrome used (e.g. CD4-FITC).

☐ The axis scales are clearly visible. Include numbers along axes only for bottom left plot of group (a 'group' is an analysis of identical markers).

☐ All plots are contour plots with outliers or pseudocolor plots.

☐ A numerical value for number of cells or percentage (with statistics) is provided.

Methodology

Sample preparation	*Describe the sample preparation, detailing the biological source of the cells and any tissue processing steps used.*
Instrument	*Identify the instrument used for data collection, specifying make and model number.*
Software	*Describe the software used to collect and analyze the flow cytometry data. For custom code that has been deposited into a community repository, provide accession details.*
Cell population abundance	*Describe the abundance of the relevant cell populations within post-sort fractions, providing details on the purity of the samples and how it was determined.*
Gating strategy	*Describe the gating strategy used for all relevant experiments, specifying the preliminary FSC/SSC gates of the starting cell population, indicating where boundaries between "positive" and "negative" staining cell populations are defined.*

☐ Tick this box to confirm that a figure exemplifying the gating strategy is provided in the Supplementary Information.

Magnetic resonance imaging

Experimental design

Design type	*Indicate task or resting state; event-related or block design.*
Design specifications	*Specify the number of blocks, trials or experimental units per session and/or subject, and specify the length of each trial or block (if trials are blocked) and interval between trials.*
Behavioral performance measures	*State number and/or type of variables recorded (e.g. correct button press, response time) and what statistics were used to establish that the subjects were performing the task as expected (e.g. mean, range, and/or standard deviation across subjects).*

Acquisition

Imaging type(s)	*Specify: functional, structural, diffusion, perfusion.*
Field strength	*Specify in Tesla*
Sequence & imaging parameters	*Specify the pulse sequence type (gradient echo, spin echo, etc.), imaging type (EPI, spiral, etc.), field of view, matrix size, slice thickness, orientation and TE/TR/flip angle.*
Area of acquisition	*State whether a whole brain scan was used OR define the area of acquisition, describing how the region was determined.*

Diffusion MRI ☐ Used ☐ Not used

Preprocessing

Preprocessing software	*Provide detail on software version and revision number and on specific parameters (model/functions, brain extraction, segmentation, smoothing kernel size, etc.).*

Normalization

If data were normalized/standardized, describe the approach(es): specify linear or non-linear and define image types used for transformation OR indicate that data were not normalized and explain rationale for lack of normalization.

Normalization template

Describe the template used for normalization/transformation, specifying subject space or group standardized space (e.g. original Talairach, MNI305, ICBM152) OR indicate that the data were not normalized.

Noise and artifact removal

Describe your procedure(s) for artifact and structured noise removal, specifying motion parameters, tissue signals and physiological signals (heart rate, respiration).

Volume censoring

Define your software and/or method and criteria for volume censoring, and state the extent of such censoring.

Statistical modeling & inference

Model type and settings

Specify type (mass univariate, multivariate, RSA, predictive, etc.) and describe essential details of the model at the first and second levels (e.g. fixed, random or mixed effects; drift or auto-correlation).

Effect(s) tested

Define precise effect in terms of the task or stimulus conditions instead of psychological concepts and indicate whether ANOVA or factorial designs were used.

Specify type of analysis: ☐ Whole brain ☐ ROI-based ☐ Both

Statistic type for inference
(See Eklund et al. 2016)

Specify voxel-wise or cluster-wise and report all relevant parameters for cluster-wise methods.

Correction

Describe the type of correction and how it is obtained for multiple comparisons (e.g. FWE, FDR, permutation or Monte Carlo).

Models & analysis

n/a	Involved in the study
☐	☐ Functional and/or effective connectivity
☐	☐ Graph analysis
☐	☐ Multivariate modeling or predictive analysis

Functional and/or effective connectivity

Report the measures of dependence used and the model details (e.g. Pearson correlation, partial correlation, mutual information).

Graph analysis

Report the dependent variable and connectivity measure, specifying weighted graph or binarized graph, subject- or group-level, and the global and/or node summaries used (e.g. clustering coefficient, efficiency, etc.).

Multivariate modeling and predictive analysis

Specify independent variables, features extraction and dimension reduction, model, training and evaluation metrics.